Heat transfer from plates to conductors : from Toroidal Field Model Coil tests analysis to ITER model

S. Nicollet*, J.L. Duchateau*, P. Hertout*

* Association Euratom-CEA, CEA/DSM/DRFC, CEA-Cadarache, F-13108 Saint-Paul-lez-Durance cedex (France)

During a safety discharge of Toroidal Field type magnets, eddy currents and associated heat generation are induced in the plates. A model has been developed from the thermohydraulic code Gandalf with introduction of the equations of the heat diffusion from plates to conductors through the steel and insulation. The comparison of calculation and experimental results for the ITER Toroidal Field Model Coil is presented.
Preliminary analysis for the ITER Toroidal Field Coils is also presented, taking into account the conductor parameters, the magnetic field and the external hydraulic circuit. The possible quench of the magnetic system is discussed.

Keywords: Cable-In-Conduit Conductors (A), Forced flow (C), Fusion magnets (F)

Nomenclature

B	Magnetic Field (T)
cp	Specific heat (J/kgK)
d	Filament diameter (m)
Dh	Hydraulic diameter (m)
E	Energy (J)
I	Current (A)
J	Current density (A/mm^2)
L	Length (m)
M	Mutual inductance (μH)
N	Number of turn in the coil
P	Power (W)
r	Radial abscisse (m)
R	Resistance ($\mu\Omega$)
S	Section in the conductor (m^2)
t	Time (s)
T	Temperature (K)
U	Perimeter (m)
V	Volume (m^3)
x	Linear abscisse (m)

Greek

α	Proportionality coefficient
δ	Elementary variation
φ	Flux (W/m^2)
λ or K	Thermal conductivity (W/mK)
μ_0	Permitivity
ρ	Density (kg/m^3)
τ	safety discharge time constant (s)
nτ	Cable time constant (ms)

Subscripts

0	initial
b	bundle
c	conductive
cl	coupling losses
eff	effective
h	hole
He	helium
hl	hysteretic losses
ins	insulation
noncu	Non Copper
p	Plates
strand	Strands
v	volumetric

Introduction

The Toroidal Field type magnets include Cable-In-Conduit Conductor (CICC) inserted into stainless steel radial plates (Figure 1). During a safety discharge of the magnet, eddy currents and associated heat generation are induced in these plates. This power is transferred into the conductor helium channels by a diffusion process through the conductor steel and insulation.

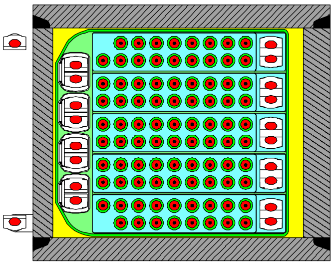

Figure 1 TFMC outer leg equatorial cross section

ITER Toroidal Field Model Coil during a safety discharge at 25 kA with 3.55 s time constant

Heat Diffusion Model

To perform the study of heat diffusion, the system (Figure2) is modelled by 3 concentric zones : the Cable-In-Conduit Conductor, the conductor insulation and the stainless steel plates.

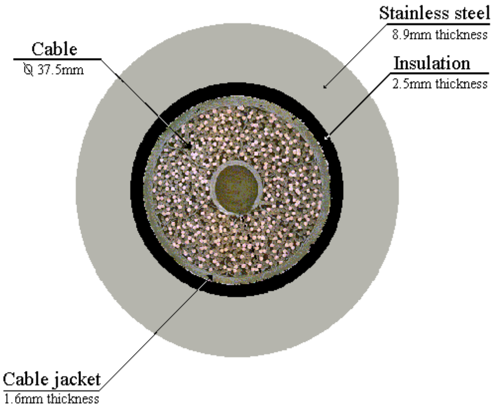

Figure 2 The TFMC model for heat diffusion

The Gandalf code is used and provides the temperature of the jacket of the Cable-In-Conduit Conductor at each time step as well as the helium temperature, pressure and mass flow rate [1].

The insulation of conductor is made of 6 layers of a glass/ kapton sandwich tape impregnated with epoxy. The thermal properties of these material are taken in [2]. The thermal conductivities of the different materials are plotted in Figure 3 and the specific heat presented in Figure 4. The conductivity of the insulation is difficult to evaluate because of the large number of interfaces and associated contact thermal resistances. Nevertheless we consider three different systems: the fiberglass, the epoxy resin and a last system which represents the values of fiberglass divided by 6 and indicated in Figure 3 and 4 as TFMC thermal conductivity.

A 1D axial symmetric geometry is considered where the heat conduction parallel to the conductor axis is neglected and the heat diffusion equation could be written for each zone :

$$r.c_p(T).\left(\frac{\partial T(r,t)}{\partial t}\right)=\left(\frac{\partial l(r)}{\partial r}+\frac{l(r)}{\partial r}\right).\frac{\partial T}{\partial r}+l(r).\frac{\partial^2 T}{\partial r^2}+P_{pv}(r,t) \quad (1)$$

The volumetric heat source in the plates is determined from the computed Joule power P_p[3] in the radial plates based on a transformer model and their total volume V_{tot} = 1.24 m^3. The power dissipated in the conductor [4] comprises the hysteretic losses P_{hl} and the coupling losses P_{cl}

$$P_p=\frac{N^2.M^2{}_{cp}}{R_p}.\left(\frac{\partial I}{\partial t}\right)^2=0.00285.\left(\frac{\partial I}{\partial t}\right)^2 \quad (2)$$

$$P_{hl}=\frac{2}{3.p}.d_{eff}.S_{nonCu}.\int J_{nonCu}(x,t).\frac{\partial B(x)}{\partial t}.dx=a(\mathrm{Im}\,ax)\frac{\partial I}{\partial t} \quad (3)$$

$$P_{cl}=\frac{1}{m_0}.(nt).S_{strands}.\int\left(\frac{\partial B(x)}{\partial t}\right)^2.dx=1.024.10^{-4}.\left(\frac{\partial I}{\partial t}\right)^2 \quad (4)$$

The total energy deposited due to the eddy currents is:

$$E_p=\int_0^\infty P_{v0}.e^{2t/t_d}.V_p=\frac{P_{v0}.t_d}{2}.V_p$$

The heat equations (1) for each material are solved using a finite difference method with a fully implicit scheme in time.In all materials, the initial temperature is T0=4.5 K and it is assumed that there is no heat flux outside the radial plates, so that $\lambda_p.(\delta T_p/\delta r) = 0$. The inner boundary condition provides the coupling between the Gandalf code and the 1D model which computes the thermal conductive flux φ_c at any point along the conductor on the inner side of the insulation: $\varphi_c = -\lambda_{ins}.(\delta T_{ins}/\delta r)$.

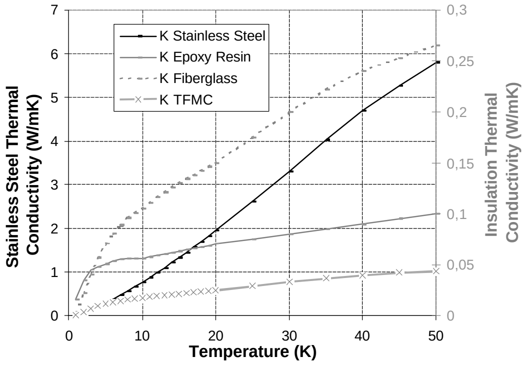

Figure 3 Thermal conductivities of TFMC Stainless Steel and Insulation

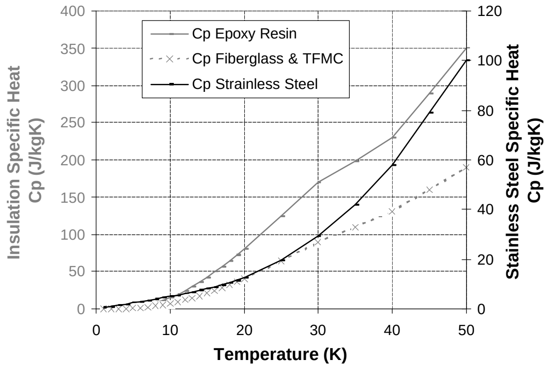

Figure 4 Specific heat of TFMC Stainless Steel and Insulation

The Toroidal Field Model Coil Results

The model was tested for a TFMC fast discharge at 25 kA, on the second pancake P1.2 of the first double pancake. The hydraulic parameters of the TFMC type cable are detailed in Table 1. The characteristics necessary to calculate the losses are presented in Table 2. The external hydraulic circuit taken into account for the TFMC is presented in Figure 5.

The energy induced by eddy currents during a 25 kA fast discharge with 3.55 s time constant is 23.9 kJ per pancake. Experimentally, only the inlet and outlet pancake temperatures are available. The results calculated with the diffusion code coupled with Gandalf are also presented in Figure 6 for the three different values system considered for the insulation. The fiberglass thermal conductivity gives an outlet temperature which doesn't agree with experimental results. The Epoxy resin thermal conductivity gives much better results and the so called TFMC thermal conductivity gives the optimum agreement between calculated results and experience. The energy corresponding to the plates losses is deposited after a time delay because of the diffusion time through the insulation [5]. This time delay is greater when the thermal conductivity is decreased.

Table 1 Hydraulic characteristics for the TF Model and ITER TF Coils

	TFMC	TF
Conductor outer diameter (mm)	40.8	43.4
Cable cross section without jacket (mm^2)	1097.2	1269.
Central hole hydraulic diameter Dhh (mm)	11.83	6
Helium section in central hole Aheh (mm^2)	109.9	28.27
Total strands cross section (mm^2)	579.1	761.5
Helium section in bundle region Aheb (mm^2)	355.2	407.4
Bundle wetted perimeter Ub (m)	3.193	3.566
Bundle region hydraulic diameter Dhb (mm)	0.445	0.457
Bundle void fraction (%)	36.85	33.4
Length (m)	82.99	375

Table 2 Characteristics for losses calculation for the TF Model and ITER TF Coils ** not considered*

	TFMC	TF
Fast discharge time (s)	3.55	11
Current initial Intensity (kA)	25	68
Non copper section S_{noncu} (mm²)	148	208.7
Strand section S_{strand} (mm²)	371	761.5
Plates total volume V_p (m^3)	1.24	154
Initial volumetric plates eddy currents Power P_{v0} (MW/m^3)	0.1082	3.024
Plates Energy per pancake E_p (kJ)	23.9	9500
Cable time constant $n\tau$ (ms)	100	*
Filament effective diameter d_{eff} (μm)	36	*
Mutual inductance M_{cp}. One Coil turn/total plates circuit (μH)	2.878	3.048
Total resistance of plates R_p ($\mu\Omega$)	27.993	3.743
Number of turns in the Coil N	98	18*134
α(I) : TFMC @25 kA	0.44	*

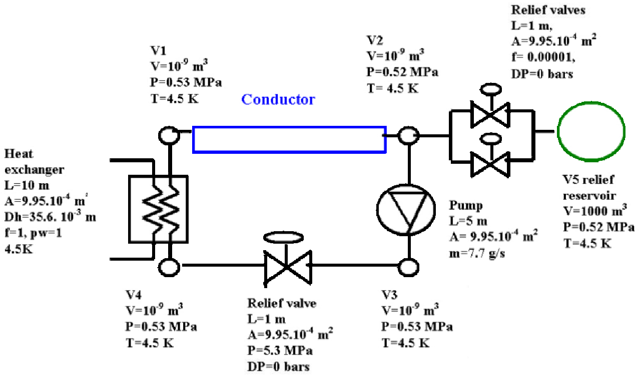

Figure 5 The TFMC external cooling circuit

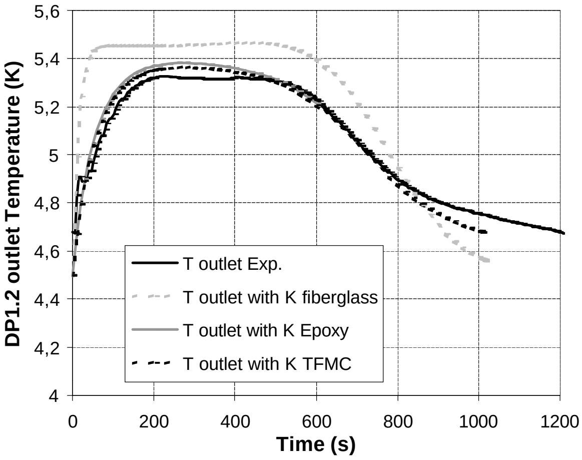

Figure 6 The TFMC P1.2 outlet temperature

ITER Toroidal Field Coil during a safety discharge at 68 kA with 11 s time constant

The ITER Toroidal Field Coil modelisation

The fast discharge of the Toroidal Field Coil of ITER is of the same type compared to the TFMC fast discharge. The main differences are the external hydraulic circuit and the order of magnitude of the conductor length and of the power induced by the eddy currents. The CICC used is of the same type.

The hydraulic circuit presented in Figure 7 shows the situation after detection of a quench : the pump is disconnected and the helium is evacuated when the pressure overcomes a certain value of 1.6 MPa through relief valves to a relief volume. The rough model presented here is based on the circuit studied by Shatil [6] in option 4 with some modifications : only one pancake is modelised with the Gandalf code instead of the whole coil and the energy deposited is known more accurately. It is supposed that the 216 plates of the 18 TF coils receive all the same energy. The relief reservoir for one pancake should then be 216 times smaller.

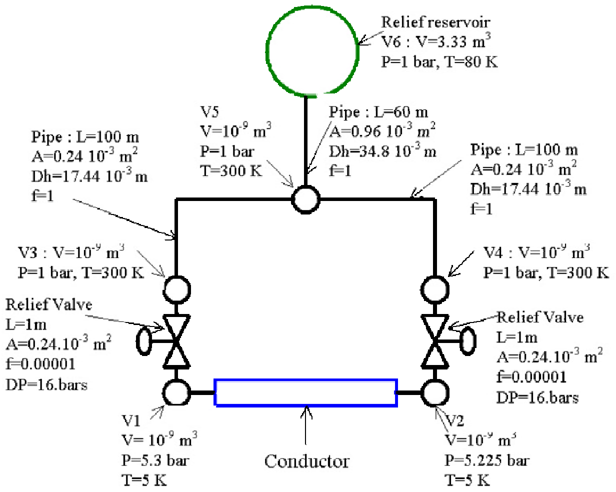

Figure 7 The ITER TF external cooling circuit

Concerning the pipes, they are supposed to conserve the same length and the same pressure drop. The mass flow rate being divided by 216, their hydraulic diameters should then be divided by $216^{2/5}$ = 8.6. The hydraulic circuit presented comprises relief valves which maintain a pressure drop across the valve of 1.6 MPa. All the values taken into account are summarized in Figure 7.

The ITER Toroidal Field Coil results

The energy induced by plates eddy currents during a 68 kA fast discharge with 11 s time constant is 9.5 MJ per pancake. The AC losses are not taken into account because they represent only a few percent of the eddy currents energy.

We perform the TF studies with the two appropriate insulation thermal conductivity systems found in the TFMC study : the epoxy resin and then the so called TFMC thermal conductivity.

In the case of epoxy resin, a quench of the conductor occurs 10 s after beginning of the safety discharge and induces a heat generation (Figure 8). The Joule energy due to the quench is 0.5 MJ. The total energy for a TF Coil is then 120 MJ. The energy deposited induces helium pressure and temperature rises (Figure 9 and 10).

The maximum pressure reached is 7.5 MPa, 25 s after the beginning of the fast discharge. After the quench which occurs at the inlet of the conductor, where the magnetic field is greater, the helium temperature presents an important rise from 10 up to 20 K. Then, this temperature seems to reach a stable value of 40 K, 150 s after beginning of the fast discharge. At the same time, the plates temperature reaches 45K after a peak at 50 K. As for the TFMC, it will take several hundreds of seconds for the total energy to be extracted from the helium and conductor.

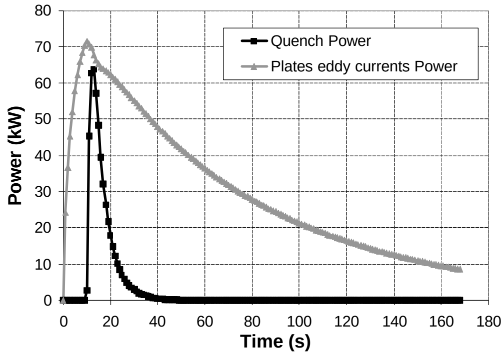

Figure 8 The ITER TF power during a safety discharge and a quench @ 68 kA with epoxy thermal conductivity

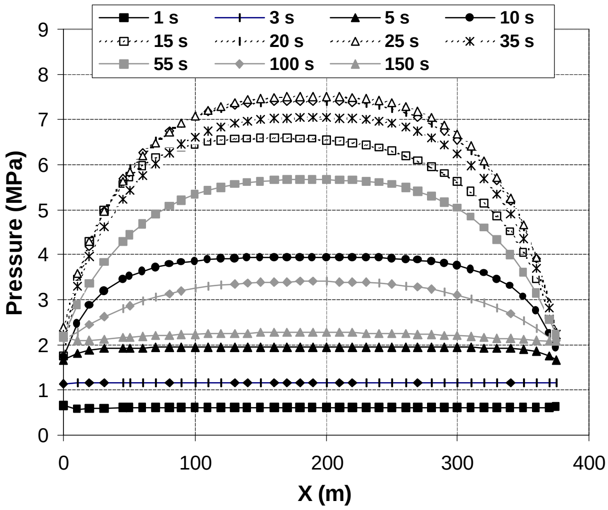

Figure 9 The ITER TF pressure after a safety discharge and a quench @ 68 kA with epoxy thermal conductivity

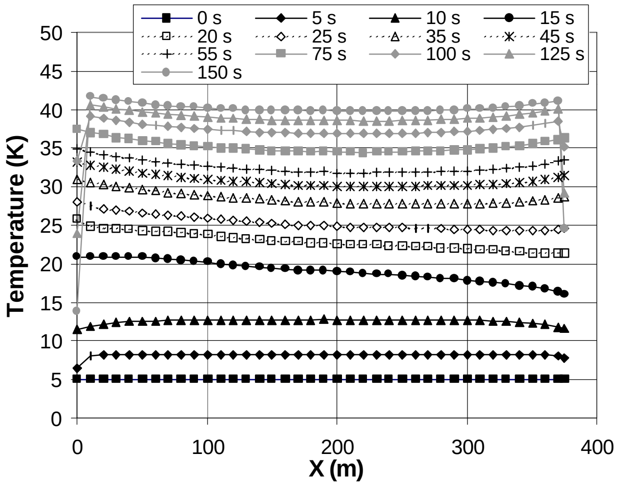

Figure 10 The ITER TF temperature after a safety discharge and a quench @ 68 kA with epoxy thermal conductivity

In the case of application to the TF of the optimal thermal conductivity found for the TFMC, the energy deposited due to the eddy currents passes through the insulation with a greater delay time ; the power peak is reduced to 28 kW (Figure 11). The conductor has only a smooth quench at 35 s after beginning of the fast discharge, and the deduced energy is 3.5 kJ. The helium pressure and temperature rises are also less important. The maximum pressure reached is 4.5 MPa at 55 s after the beginning of the quench (Figure 12). The temperature is established slower near 35 K (Figure 13).

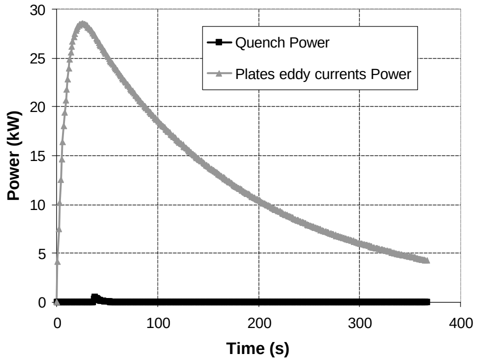

Figure 11 The ITER TF power during a safety discharge and a smooth quench at 68 kA with TFMC optimal thermal conductivity

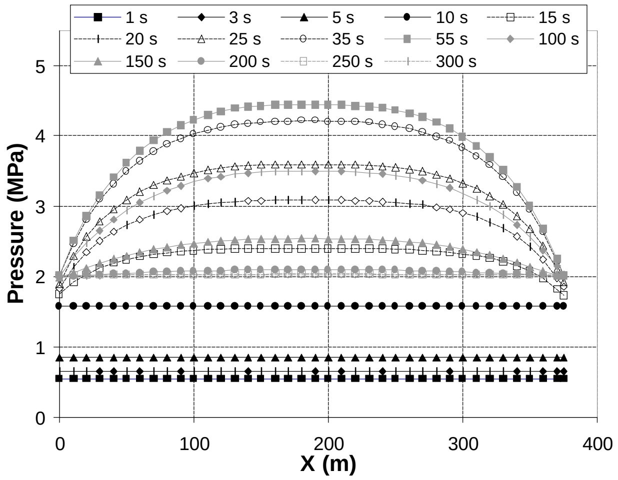

Figure 12 The ITER TF pressure after a safety discharge and a quench at 68 kA with TFMC optimal thermal conductivity

For an even greater value system of insulation thermal conductivity (fiberglass), the quench occurs earlier, at 5 s and the maximum pressure reached is 10.0 MPa. In the most relevant studied cases, the quench of the conductor occurs at a time delay (10 s for epoxy resin and 35 s for TFMC thermal conductivity) greater than the value of 7 s indicated by Shatil [6]. In our case the energy deposited due to the quench is lower and the pressure remains therefore lower than 7.5 MPa, a much more acceptable value compared to Shatil calculations of 12.0 MPa at 15 s. This demonstrates the important role played by the insulation thermal conductivity during the TFMC and TF conductors safety discharge. Further studies and specially thermal conductivity measurements are foreseen to characterise this parameter.

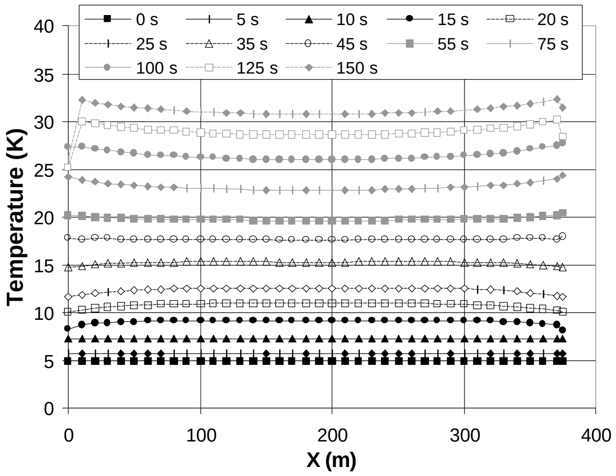

Figure 13 The ITER TF temperature after a safety discharge and a quench at 68 kA with TFMC optimal thermal conductivity

Conclusion

The TFMC and the ITER TF fast discharges were analysed. The deposited energy and the pressure and temperature rises were presented. The diffusion time of energy from plates to helium during the safety discharge was studied using the thermal hydraulic code Gandalf and a cylindrical model for heat diffusion. This model has shown the importance of the thermal conductivity of insulation on the diffusion phenomenon. In fact, in the case of the TF fast discharge, this parameter is driving the quench of the conductor and so all the helium pressure and temperature responses.

References

1. L. Bottura et al., A numerical model for the simulation of quench in the ITER magnets, Journal of computational Physics 125, 1996, pp. 26-41.
2. ITER Design description document N11 DDD 156 01-07-13 R0.1.
3. P. Hertout et al., Model of heat deposition during fast discharge tests of the ITER TFMC, IEEE Transactions on applied Superconductivity, vol.12, N°1, march 2002, pp. 1426-1429.
4. J.L. Duchateau et al., AC losses in the ITER TF model Coil : a comparison between model and experimental results, 19th Int. Cryogenic Engineering Conference, Grenoble, France, July 2002, to be published.
5. J.L. Duchateau et al., ITER Toroidal Field Model Coil test : analysis of heat transfer from plates to conductors, Symposium On Fusion Technology, Helsinki, Sept. 2002, to be presented.
6. N. Shatil, ITER Design Description Document, Conductor Design and Analysis, Annex 10 : Thermo-hydraulic Analysis of the TF, CS and PF Magnets, Attachment 5, 2002